Histone Deacetylase Inhibitor Panobinostat Induces Clinical Responses with Associated Alterations in Gene Expression Profiles in Cutaneous T-Cell Lymphoma

Leigh Ellis,[1,11] Yan Pan,[2] Gordon K. Smyth,[3] Daniel J. George,[5] Chris McCormack,[1,2,4] Roxanne Williams-Truax,[5] Monica Mita,[6] Joachim Beck,[7] Howard Burris,[8] Gail Ryan,[1] Peter Atadja,[9] Dale Butterfoss,[9] Margaret Dugan,[10] Kenneth Culver,[10] Ricky W. Johnstone,[1,4] and H. Miles Prince[1,4]

Abstract

Purpose: Histone deacetylase inhibitors can alter gene expression and mediate diverse anti-tumor activities. Herein, we report the safety and activity of the histone deacetylase inhibitor panobinostat (LBH589) in cutaneous T-cell lymphoma (CTCL) and identify genes commonly regulated by panobinostat.

Experimental Design: Panobinostat was administered orally to patients with CTCL on Monday, Wednesday, and Friday of each week on a 28-day cycle. A dose of 30 mg was considered excessively toxic, and subsequent patients were treated at the expanded maximum tolerated dose of 20 mg. Biopsies from six patients taken 0, 4, 8, and 24 h after administration were subjected to microarray gene expression profiling and real-time quantitative PCR of selected genes.

Results: Patients attained a complete response ($n = 2$), attained a partial response ($n = 4$), achieved stable disease with ongoing improvement ($n = 1$), and progressed on treatment ($n = 2$). Microarray data showed distinct gene expression response profiles over time following panobinostat treatment, with the majority of genes being repressed. Twenty-three genes were commonly regulated by panobinostat in all patients tested.

Conclusions: Panobinostat is well tolerated and induces clinical responses in CTCL patients. Microarray analyses of tumor samples indicate that panobinostat induces rapid changes in gene expression, and surprisingly more genes are repressed than are activated. A unique set of genes that can mediate biological responses such as apoptosis, immune regulation, and angiogenesis were commonly regulated in response to panobinostat. These genes are potential molecular biomarkers for panobinostat activity and are strong candidates for the future assessment of their functional role(s) in mediating the antitumor responses of panobinostat.

Cutaneous T-cell lymphomas (CTCL) are extranodal non-Hodgkin's lymphomas that are characterized by the accumulation of clonal T lymphocytes in the skin (1, 2). The most common variants are mycosis fungoides and the leukemic variant, Sezary syndrome. The lesions of patients with mycosis fungoides with early-stage disease (patch or plaques with no tumor or nodal/visceral involvement) are generally well controlled with skin-directed therapies such as photo-therapy or topically applied corticosteroids (3). Advanced-stage skin disease such as tumor lesions or erythroderma, nodal/visceral disease require biological response modifiers such as IFN-α, retinoids, denileukin diftitox, or multiagent chemotherapy; recently, the histone deacetylase inhibitor (HDACi) vorinostat (Zolinza) has been approved by the U.S. Food and Drug Administration for the treatment of CTCL (4). Although partial and complete remission can be

Table 1. Responses following treatment with panobinostat

ID	Treatment duration (wk)	Dose (mg)	Biopsy for correlative studies	Response		
				PGA (days to onset)	PGA (best response)	CA (days to onset)
101	4	30	Yes	PR (105)	0	PR (62)
102	10	20	Yes	SD	5	SD
103	24	20	Yes	PR (106)	0	PR (106)
104	14	20	Yes	PR (57)	3	SD
105	14	20	Yes	PD	5	N/A§
106	8	20	Yes	SD	4	SD
107	116	20	No	PR (113)	2	N/A§
109	4	20	No	PD	6	SD
110	38	20	No	PR (57)	2	PR (57)
111	36	20	No	PR (28)	1	PR (85)

*Other non-drug-related toxicity: grade 3 atrial fibrillation (see text).
†CR occurred 167 days following last dose of LBH.
‡Due to grade 2 fatigue.
§Total body involvement at baseline response based solely on PGA.
‖Due to progressive disease on study.

achieved, subsequent relapses are common and curative therapy remains elusive (3, 5–8).

HDAC are enzymes that regulate chromatin structure and function through the removal of acetyl groups from lysine residues of core histones, facilitating a closed chromatin state and transcriptional repression (9). The opposing activities of HDAC and histone acetyltransferases regulate histone acetylation and chromatin architecture (9). There is growing evidence that epigenetic changes play a crucial role in cancer onset and progression, and it has been widely recognized in recent years that HDAC are promising targets for therapeutic interventions intended to reverse aberrant epigenetic states associated with cancer (10–13).

HDACi are a new class of chemotherapeutic drug shown in preclinical studies to have potent anticancer activities (9, 13). Although it is not yet clear exactly how HDACi achieve therapeutic anticancer responses, these agents induce rapid histone hyperacetylation and chromatin remodeling and can activate or repress genes regulating apoptosis, proliferation, differentiation, angiogenesis, and immune responses (9). Panobinostat (LBH589) is a novel HDACi that belongs to the cinnamic hydroxamic acid class of compounds (14). Panobinostat is formulated as both an oral capsule and an i.v. solution currently undergoing phase I trials (13). Two other HDACi, romidepsin (depsipeptide) and suberoylanilide hydroxamic acid (vorinostat), have been recognized to induce disease regression in CTCL (15–17). The therapeutic action of HDACi in CTCL patients may relate to induction of histone hyperacetylation, altered gene expression, and subsequent apoptosis of malignant T cells (18), although other effects such as loss of cell proliferation and decreased angiogenesis may also play a role (19).

We are conducting an ongoing phase I, open-label, dose-escalation study in patients with solid tumors and non-Hodgkin's lymphoma with the primary objective of evaluating the safety, tolerability, biologic activity, and pharmacokinetic profile of oral panobinostat. That ongoing study investigates various schedules of panobinostat, one of which is the Monday/Wednesday/Friday (MWF) schedule presented here (20). Moreover, in this particular cohort, we accrued patients with CTCL and we present the results of these CTCL patients in this article. We recognized we had an entirely unique opportunity in this study to examine for the first time serial changes in tumor acetylation status and gene expression following HDACi administration by performing repeated tumor biopsies at short time intervals, something not possible in patients with systemic or internal tumors. Moreover, this was a group of patients who showed responses to the HDACi therapy. Thus, using biopsy samples from patients on study, we did microarray-based gene expression profiling studies and assessed panobinostat-mediated histone hyperacetylation over time.

Materials and Methods

All patients signed an informed consent form and the study was approved by the institution regulatory boards. Two centers (Peter MacCallum Cancer Centre and Duke University Medical Center) were involved in enrolling this subset of patients with CTCL.

Patient eligibility. Patients at least 18 years old with cytopathologically confirmed CTCL whose disease had progressed despite standard therapy or for whom no standard therapy exists were eligible. Inclusion was irrespective of stage of disease or extent of prior therapy. Patients were also required to have an Eastern Cooperative Oncology Group performance status score of ≤2 and a life expectancy of >12 weeks. All patients were required to have an absolute neutrophil count ≥1.5 × 10^9/L, hemoglobin ≥90 g/L, and platelets ≥100 × 10^9/L. Potassium, total calcium, magnesium, and phosphorus levels needed to be equal or above the lower limit of normal or correctable with supplements. Patients were excluded from the study if there was impaired cardiac function, clinically significant cardiac diseases, or congenital prolonged QT syndrome.

Study design. This study is a part of an ongoing phase I, multicenter, dose-escalation study of panobinostat (Novartis) administered orally on two dose schedules in adult patients with advanced solid tumors or non-Hodgkin's lymphoma. The primary objective of this study was to determine the maximum tolerated dose and dose-limiting toxicity

Table 1. Responses following treatment with panobinostat (Cont'd)

			Response		
Best response	Time to response (d)	Time to progression (d)	Overall survival	Reason for discontinuation	Follow-up (months since initiation)
CR* (172) [†]	62	252	368	Adverse event (grade 3 diarrhea)	12
SD	N/A	79	1,109+	Disease progression	23
CR (190)	106	338	9,711+	Subject withdrew consent [‡]	22
PR	57	106	545	Adverse event (grade 3 diarrhea)	4
PD	N/A	103	1,010+	Disease progression	5
SD	N/A	56	871+	Adverse event (prolonged cytopenia)	3
N/A	113	794	1,001+	Disease Progression	27
PD	N/A	27	48‖	Disease progression	2
PR	57	256	844+	Disease progression	10
PR	28	254	259+	Disease progression	9

(DLT) of oral panobinostat when administered as a single agent to adult patients. Additionally, the study was designed to characterize the safety, tolerability, biologic activity, and pharmacokinetic profile of oral panobinostat when administered to this patient population.

Oral panobinostat was administered as 5 or 20 mg hard gelatin capsules. The starting dose was 15 mg with potential escalation to 20, 30, and 40 mg. In this part of the study, panobinostat was administered orally once daily on Monday, Wednesday, and Friday of each week on a 28-day cycle. The dose of 30 mg was deemed the DLT dose of a MWF schedule and subsequent patients were treated at the expanded maximum tolerated dose of 20 mg (20). DLT toxicity was defined as an adverse event or abnormal laboratory value assessed as unrelated to disease progression, intercurrent illness, or concomitant medications and occurs during the first 28 days following the first dose of oral panobinostat in cycle 1 and met any of the criteria according to National Cancer Institute Common Terminology Criteria for Adverse Events version 3.0. Patients continued treatment with oral panobinostat until the patient experienced unacceptable toxicity that precluded any further treatment or disease progression.

Patient evaluation/pretreatment evaluation. Dermatologic assessment was carried out at baseline, day 1 of each cycle, and at the time of treatment completion, measuring the body surface area involvement by patch and plaque. Photographs of index lesions were taken at baseline and at every scheduled visit using standardized methods. The CTCL regional index and index lesion photographs and postbaseline histologic analyses of any CTCL lesion biopsy specimens obtained served as supporting data to the efficacy endpoint evaluations. Pretreatment evaluation included routine biochemical and hematology profile (full blood exam) including blood film and flow cytometry for assessment of circulating Sezary cells. Assessment of extracutaneous involvement by imaging studies included chest X-ray, cardiac imaging (multiple-gated acquisition scan or echocardiogram), chest, abdomen, and pelvic computed tomographic scan with contrast, and [^{18}F]fluorodeoxyglucose positron emission tomography as clinically indicated. Bone marrow aspirate and biopsy were done in all patients.

Response/on-treatment and post-treatment evaluation. Patients were evaluated at day 1 of each cycle before administration of oral panobinostat with laboratory tests; additionally, a full blood exam was repeated on days 8, 10, 15, 17, 22, and 24 of cycle 1 as well as day 15 of cycle 2 and each subsequent cycle. Coagulation profile was obtained on day 1 of cycle 2 or repeated at least once while receiving study drug. Hepatic and renal function tests were done on days 8, 15, and 22 of cycle 1 and 2 and day 15 of cycle 3 and each subsequent cycle.

Skin lesion response was completed using the Physician's Global Assessment of Clinical Condition (PGA; Supplementary Table S1) and Composite Assessment of Index Lesion Disease Severity (CA; ref. 5). Response by a PGA from baseline represented the investigator's

assessment of the overall extent of improvement or worsening of the patient's cutaneous disease compared with baseline. A clinical partial response (PR) required at least 50% improvement and a clinical complete response (CR) required 100% improvement (histologic confirmation not required). The CA efficacy endpoint had two separate components based on up to 5 representative index lesions using a 0 to 8 scale to independently assess scaling, erythema, plaque elevation, and hypopigmentation or hyperpigmentation. In addition, the surface area of each index lesion was calculated by multiplying the maximal bidirectional diameters of each index lesion. The sum of all measurements (scores) were summed and added to the sum for all clinical signs to establish the CA score at baseline. At each subsequent evaluation, the sum of these variables was divided by the baseline CA. A CA ratio ≤ 1.0 indicates improvement in disease and a CA ratio ≥ 1.0 indicates a worsening of disease. A clinical CR required that the CA ratio = 0 without confirmatory biopsy. PR is defined as a CA ratio ≤ 0.5. Improvement in the PGA and CA index required confirmation by at least two consecutive observations separated by at least 4 study weeks before a patient could be classified as a responder. Clinical progressive disease (PD) requires worsening of disease compared with baseline by >25% and/or ≥50% increase in the sum of the products of the abnormal lymph nodes and visceral disease from baseline or from the on-study nadir (which ever is smaller) for PGA. PD is defined as 50% increase from best response (nadir) of the CA ratio or score. Patients in whom PD developed before a response occurred were classified as having PD even in the event of later improvement. A patient was classified as a responder if that patient met response criteria for either the PGA or the CA endpoint. Patients with total body involvement with mycosis fungoides were classified as responders based solely on PGA endpoints. Patients who came off panobinostat for reasons other than disease progression continued to be monitored on a monthly basis with physical examination and routine full blood exam and biochemistry with imaging done if disease progressed according to local investigator methodology, which was to approximate the protocol-specified times.

Statistical analysis. All patients who received one dose of panobinostat were included in the response and safety analyses. As the primary study objective was not hypothesis testing, rigorous sample size and power calculations were not applied. Patient demographics, safety, and disposition data are presented using descriptive statistics. Response rates were calculated with their 95% confidence intervals using the Clopper-Pearson exact method.

Detection of acetylated histone H3 by immunohistochemistry. Automated immunohistochemistry was done on sections from six CTCL patients using a DAKO Autostainer Plus (DakoCytomation Detection Systems). Sections were incubated with anti-acetyl histone H3 polyclonal antibody (1:1,200; Upstate) and then treated with EnVision+ System horseradish peroxidase anti-rabbit (DakoCytomation Detection Systems). Sections were counterstained using an in-house

formulated hematoxylin. Samples were quantitated for the level of acetylation by using Metamorph 7 (Molecular Devices).

Effect on histone acetylation in mononuclear cells. Mononuclear cells were taken post-dose 1 at 3, 8, 24, and 48 h, post-dose 2 at 48 h, and post-dose 3 at 72 h and whole-cell lysates were prepared in lysis buffer (Qiagen). Proteins (25 μg) were separated by SDS-PAGE and Western blotting was done using anti-acetyl histone H3 and histone H4 antibodies (Upstate) and with anti–glyceraldehyde-3-phosphate dehydrogenase (Upstate) to control for protein loading. Blots were incubated in Alexa Fuor 680 anti-mouse (Molecular Probes) and IRDye 800 anti-rabbit (Rockland Immunochemicals) secondary antibodies and acetylated histones were quantitated using an Odyssey detection System (Li-Cor Biosciences).

RNA purification. To ensure sample processing did not influence array data, 3-mm punch biopsies taken at the indicated times were imbedded in OCT medium and immediately snap frozen in liquid nitrogen to ensure tissue integrity. All samples were stored at -80°C and all subsequent RNA extraction or immunohistochemistry preparation

was done on the same day. Total RNA was purified from patient skin biopsies samples taken at 0, 4, 8, and 24 h post-panobinostat administration with TRIzol reagent (Invitrogen) before being applied to a Qiagen RNeasy kit according to manufacturer's instructions.

Microarray hybridization. Double-stranded cDNA was generated using a GeneChip Expression 3′-Amplification Two-Cycle Synthesis kit (Affymetrix) and biotin-labeled antisense cRNA was synthesized by *in vitro* transcription. cRNA (20 μg) was then fragmented and hybridized to a Human Genome U133A Plus 2.0 Gene Chip (Affymetrix) GeneChip. All proceeding washes, stains, and scanning protocols were done according to the manufacturer's instructions. Chips were then scanned twice using a 2500 Scanner. Data were extracted using Affymetrix GeneChip Operating Software version 1.0.

Quality assessment and normalization. Raw data for each Gene-Chip were quality assessed using a variety of graphical methods (21). These assessments led us to the discard of one array as showing insufficient signal probably because of insufficient RNA in the sample. Intensities were background corrected, normalized, and summarized

Fig. 1. Clinical effects of panobinostat. Photographs of patient 101 taken at baseline (*top*) and post-treatment with panobinostat (*bottom*) showing complete remission. Responses of erythematous plaques on the face and torso of patient 101 to treatment with panobinostat.

Fig. 2. Clinical effects of panobinostat. Photographs of patient 107 with Sezary syndrome taken at baseline (*top*) and after 8 months of treatment with panobinostat (*bottom*) with ongoing partial remission. Response of erythematous plaques with hyperkeratotic scale and fissures on the palms and feet of patient 107 to treatment with panobinostat.

at the probe-set level using the gcRMA algorithm (22) implemented in the gcRMA software package for R.[12] Probe sets not reaching a normalized intensity of $2^4 = 16$ on at least 4 of the 22 GeneChip were filtered from further analysis.

Differential expression. Analysis of individual patient gene expression was analyzed using GeneSpring GX 7.3.1 (Aligent Technologies). Raw data were initially background corrected using gcRMA algorithm. Changes in gene expression following panobinostat administration were further corrected by normalizing to the corresponding baseline arrays, and final expression analysis was finally corrected for by selecting for genes changing 2-fold in their gene expression patterns.

Differential expression analysis of genes that were altered in all patients consistently over time in response to panobinostat was done with the limma software package for R (23). An additive ANOVA model was fitted for each probe set with patient and time as the two explanatory factors. This allowed us to detect genes that respond to panobinostat while adjusting for differences between patients. The additive ANOVA finds genes that respond to panobinostat in a consistent way across the six subjects.

As there was some subtle graduation in data quality between the different RNA samples, empirical array quality weights were estimated from the expression data and incorporated into the differential expression analysis (24). This served to down-weight lesser-quality arrays, in a graduated way, improving the precision and power of the overall differential expression analysis. Differentially expressed genes were selected based on empirical Bayes *F* statistics for time across the

_____
[12] http://www.r-project.org

different schedules (25). The method of Benjamini and Hochberg (26) was used to control the expected false discovery rate of <15%.

Real-time quantitative PCR analysis. Real-time quantitative PCR was done to verify the expression of selected genes that responded to panobinostat (false discovery rate < 15%). cDNA was synthesized and consequent gene expression was analyzed as described previously (27). Primers to human *GUCY1A3* (forward 5′-CAGACGTTTAGCGGGAT-CAT-3′ and reverse 5′-CCCCAAAAACAAGATTGC-3′), *NR2F2* (forward

Fig. 3. Effects of panobinostat on histone acetylation. *A,* tumor biopsies from patients 104 and 106 were obtained directly before they received the first dose of panobinostat or at various times points (4, 8, and 24 h) following therapy. Immunohistochemistry using an anti-acetyl histone H3 antibody was done, which showed an increase in acetylated histone H3 in mononuclear cells over time following panobinostat treatment. The fold increase in acetyl histone H3 staining over background (T_0) for patients 104 and 106 in tumor biopsy samples (*B*) and isolated mononuclear cells (*C*) was quantitated as detailed in Materials and Methods.
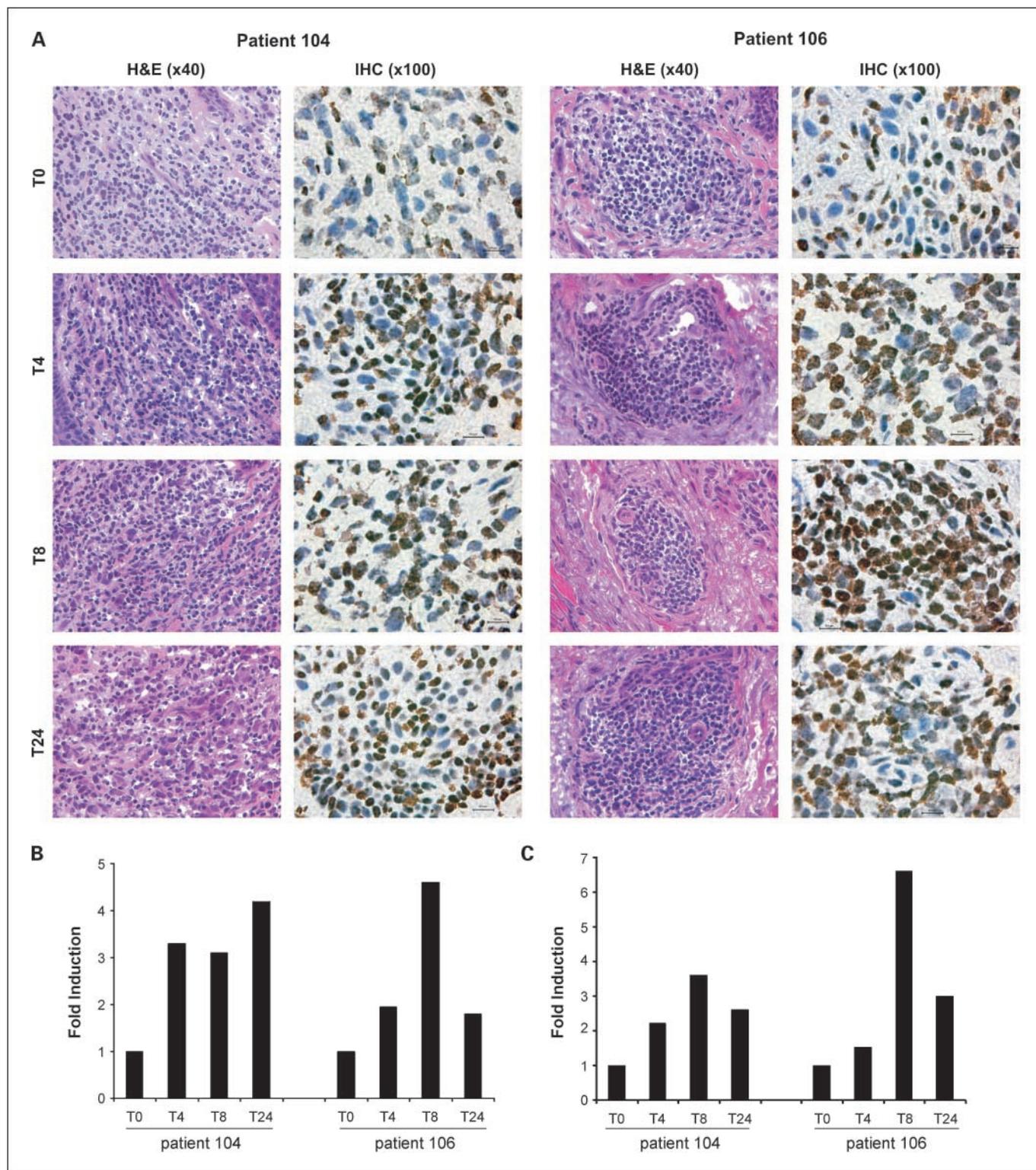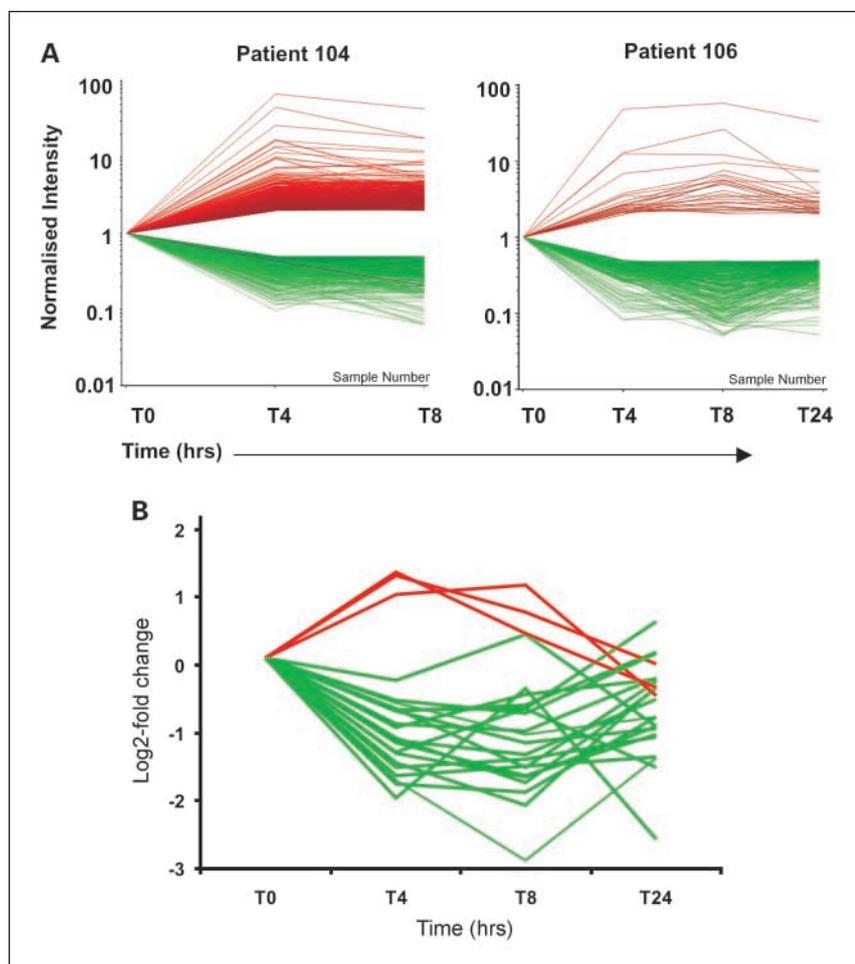
Fig. 4. Effects of panobinostat on histone acetylation. *A,* tumor biopsies from patients 104 and 106 were obtained directly before they received the first dose of panobinostat or at various times points following therapy and changes in gene expression were assessed by microarray. Genes that were differentially regulated by at least 2-fold from time 0 h to at least one later time point in response to panobinostat are shown. *Red,* up-regulated genes; *green,* down-regulated genes. Each line corresponds to a single gene. *B,* 23 genes (3 up-regulated and 20 down-regulated) were found to respond to panobinostat in all six patients tested.

5'-CGGAGGAACCTGAGCTACAC-3' and reverse 5'-CAGGTAC-GAGTGGCAGTTGA-3'), *ANGPT1* (forward 5'-GGGAGGAAAAAGA-GAGGAAGA-3' and reverse 5'-ATTCCTTCCAGCCTCTTTGG), and *CCND1* (forward 5'-AACTACCTGGACCGCTTCCT-3' and reverse 5'-CCACTTGAGCTTGTTCACCA-3') were designed using the University of California-Santa Cruz genome browser[13] and primer 3[14] Web sites. The ribosomal gene *L32* (forward 5'-TTCCTGGTCCACAACGTCAAG-3' and reverse 5'-TGTGAGCGATCTCGGCAC-3') was used as the control gene.

Results

Patient characteristics. Ten CTCL patients were registered to the study and the result of the CTCL patients are presented in detail in this article. The characteristics of these patients are described in Supplementary Table S2. This CTCL cohort was part of a larger MWF weekly dosing cohort into which 32 patients were entered and have been presented in abstract form (20). Briefly, with respect to the larger 32-patient cohort, patients received 15 mg ($n = 3$), 30 mg ($n = 10$; the DLT), or 20 mg ($n = 19$; the maximum tolerated dose). Tumor types included CTCL ($n = 10$), renal cell ($n = 6$), melanoma ($n = 6$), prostate ($n = 4$), hepatic ($n = 1$), rhabdomyosarcoma ($n = 1$), mesothelioma ($n = 1$), colon ($n = 1$), bladder ($n = 1$), and parotid gland ($n = 1$). Three DLT were reported: grade 3

diarrhea at 30 mg, transient grade 4 thrombocytopenia at 30 mg, and grade 3 fatigue at 20 mg. The most common adverse events were anorexia, nausea, fatigue, diarrhea, and transient thrombocytopenia. Panobinostat was rapidly absorbed in plasma (T_{max}, 1.5 h) and then declined with a mean terminal half-life of 16 h. C_{max} and AUC increased linearly with doses between 15 and 30 mg (20).

The median age of the CTCL patients was 59.5 years and 8 patients had advanced-stage mycosis fungoides (stage IIB or higher). One patient (101) received 30 mg MWF and the remaining 9 patients received 20 mg MWF weekly. A summary of the patients' treatment and response information is shown in Table 1. The 9 patients in the 20 mg treatment group had a median duration of panobinostat treatment of 14 weeks (range, 4-116 weeks), whereas the patient treated with 30 mg/dose with this schedule was treated for only 4 weeks due to dose-limiting diarrhea. Ultimately, 6 patients discontinued due to disease progression, 3 patients withdrew due to adverse experiences, and 1 patient withdrew consent due to a combination of grade 2 fatigue and difficulty with frequent monitoring visits.

Toxicity. Within the CTCL cohort of 10 patients, one DLT was reported: grade 3 diarrhea at 30 mg (101). The most common adverse events were anorexia, nausea, fatigue, diarrhea, and transient thrombocytopenia. The major toxicity observed was diarrhea (2 patients) seen as early as week 3. In

---

[13] http://genome.ucsc.edu

[14] http://frodo.wi.mit.edu/cgi-bin/primer3/primer3_www.cgi

patient 101, despite drug dosage reduction to 15 mg, concomitant medication administration, and hospitalization, recurrent diarrhea developed and panobinostat was discontinued. The patient, however, had ongoing improvement

without further therapy, achieving CR 167 days later (Fig. 1). Other grade 3 toxicities observed were thrombocytopenia (2 patients, both occurring during week 8 of treatment), neutropenia (2 patients), skin infection, atrial fibrillation, eye
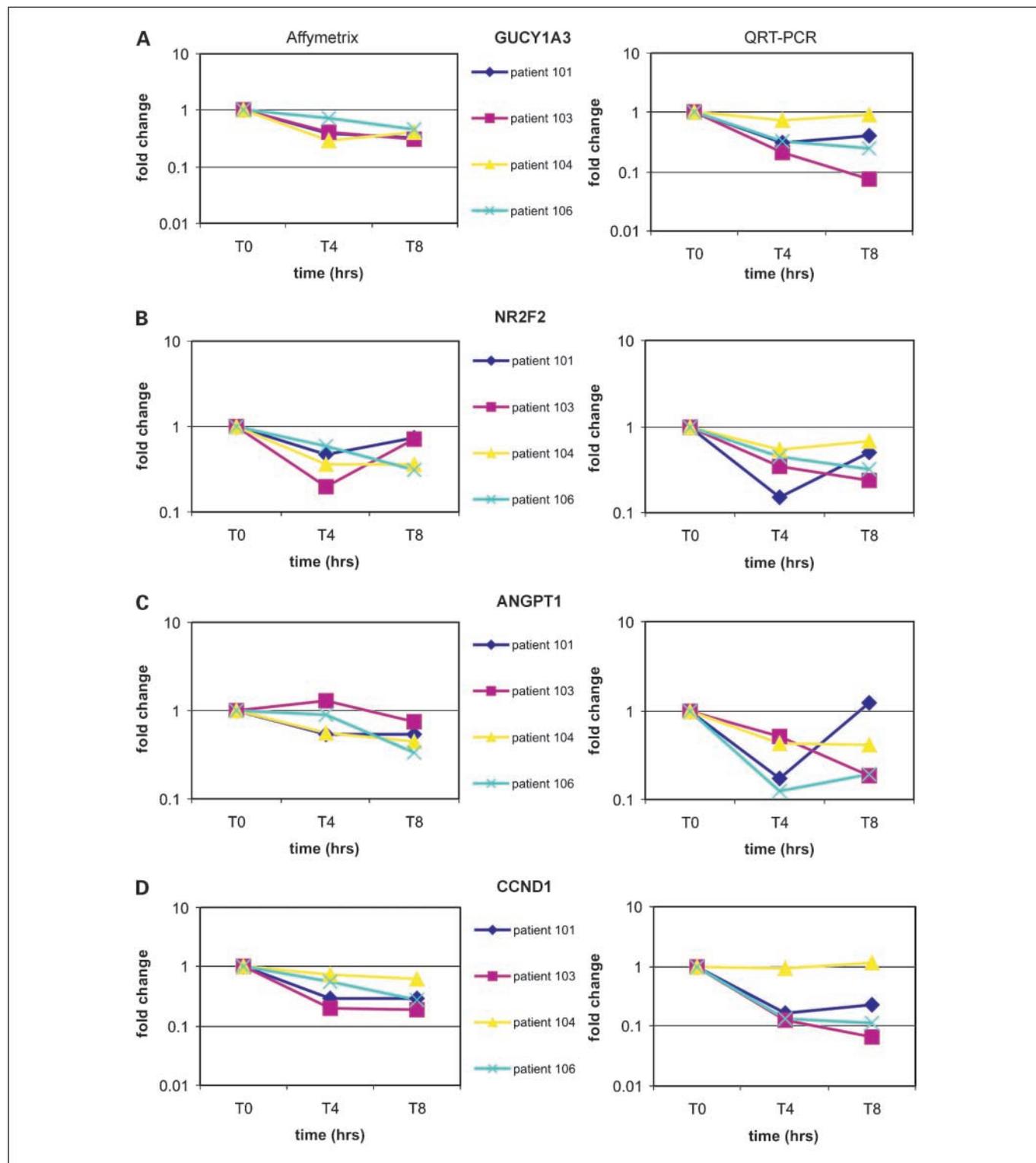

Fig. 5. Validation of microarray data by QRT-PCR. RNA from biopsy samples was obtained from patients 101, 103, 104, and 106 before panobinostat treatment or at various time points following treatment. QRT-PCR was used to detect expression of the following genes: (*A*) GUCY1A3, (*B*) NR2F2, (*C*) ANGPT1, and (*D*) CCND1, whose expression was altered in all patients tested. Values for each gene were normalized to expression levels of L32 and fold induction at each time point was calculated relative to time 0 h. *Left,* microarray data; *right,* results from QRT-PCR.

swelling, and anemia. The patient who developed atrial fibrillation developed symptoms 6 h after receiving panobinostat on day 1 of cycle 2; magnesium and potassium levels were normal. The atrial fibrillation responded rapidly to digoxin and the patient continued on panobinostat therapy. The patient had no episodes of atrial fibrillation either prior or since. One patient (103) was discontinued from the study due to grade 2 fatigue, which developed at week 12.

Clinical efficacy. Median duration of therapy was 14 weeks (range, 4-116) for all 10 patients. Responses to treatment are detailed in Table 1. Clinical efficacy was observed in 8 patients: CR was seen in 2 patients (CR was seen at both 20 and 30 mg daily dose levels; Fig. 1), 4 CTCL patients reached a PR with median time to onset of response of 57 days (28-113 days), and an additional 2 CTCL patients met the criteria for stable disease (SD). Of note, both patients achieved a CR following discontinuation of drug, one 2 weeks and the other 24 weeks following last dose of panobinostat. The median time to response was 60 days (range, 28-113). Median time to progression was 179 days (range, 27-794). Two of the 3 patients with circulating Sezary cells responded to panobinostat (Fig. 2).

Immunohistochemistry. Panobinostat-mediated histone acetylation in patient biopsy samples before and after administration of panobinostat was assessed (Fig. 3A). Hyperacetylation of histone H3 was observed in tumor cells as little as 4 h after administration of panobinostat and increased over time, whereas little histone hyperacetylation was observed in surrounding stromal cells. Histone hyperacetylation was quantified using Metamorph software and found that peak hyperacetylation levels of ~4-fold over untreated control levels were observed 4 to 8 h following therapy (Fig. 3B).

Effect on histone acetylation in mononuclear cells. To further evaluate the pharmacodyamic effect of panobinostat, 9 patients were evaluable for histone acetylation in blood mononuclear cells. Following each of MWF doses, hyperacetylation was consistently observed to 48 h (before next dose) and out to 72 h (following the Friday dose and before Monday dosing). Panobinostat induced histone acetylation in both responding and nonresponding patients, and a representative analysis of the kinetics of histone hyperacetylation in patients 104 and 106 treated during the first cycle of panobinostat is shown in Fig. 3C.

Gene expression profiling. To identify changes in gene expression following treatment with panobinostat, microarray studies using patient biopsy samples were obtained directly before treatment and at 4, 8, and 24 h following the first dose of panobinostat (day 1, cycle 1). As shown in Fig. 4A using gene expression profiles from patients 104 and 106 as examples, changes in gene expression were observed consistently at 4 h and persisted to at least 8 h for most genes. The number of genes showing a ≥2-fold change in expression in at least one time point following panobinostat treatment compared with untreated biopsy samples is as follows: patient 101 (1,358 genes changed, 12% up-regulated and 88% down-regulated), patient 103 (1,281 genes changed, 23% up-regulated and 77% down-regulated), patient 104 (1,466 genes changed, 61% up-regulated and 39% down-regulated), patient 105 (310 genes changed, 36% up-regulated and 64% down-regulated), and patient 106 (285 genes changed, 10% up-regulated and 90% down-regulated). Evidently, in most patient samples, panobinostat induced transcriptional repression of more genes than were activated.

We used a two-way additive ANOVA model and empirical Bayes F statistics to find genes showing a consistent and statistically significant response to panobinostat over time across all the patients. Twenty-three genes were significant at a false discovery rate of <15% (Fig. 4B; Supplementary Table S3). Twenty genes were repressed following panobinostat treatment, whereas only 3 genes were activated. Interestingly, genes such as IGF1 and CCND1 (encoding cyclin D1) identified previously in *in vitro* studies as HDACi-regulated genes (28, 29) were identified in our screen. Moreover, genes that mediate biological responses known to be downstream of HDAC inhibition [*Septin10*, *TEF*, and *SORBS2* (apoptosis); *NR2F2*, *CCND1*, and *TM4SF18* (cell proliferation); *GUCY1A3* and *ANGPT1* (angiogenesis); and *LAIR1* (immune modulation)] were identified. Previous studies had indicated *CDKN1A* (encoding p21$^{WAF1/CIP1}$) to be a gene readily up-regulated in response to HDACi treatment *in vitro* (30). Our data indicate that *CDKN1A* was not universally up-regulated in response to panobinostat. Patient 101 (CR), patient 103 (CR), and patient 105 (PD) displayed a slight, significantly significant increase in expression of CDKN1A, whereas patient 104 (PR) and patient 106 (SD) showed no increase in *CDKN1A* expression following treatment with panobinostat.

To validate the gene expression data obtained by microarray, QRT-PCR was used to assess the expression of selected genes from Supplementary Table S3. As shown in Fig. 5, there was a strong overlap in gene expression profiles as assessed by microarray and QRT-PCR in terms of both magnitude and kinetics of the response.

Discussion

Here, we present the results of a cohort of 10 patients with CTCL within the ongoing phase I study of the oral formulation of the HDACi panobinostat. That ongoing study investigates various schedules of panobinostat, one of which is the MWF schedule presented here. In this group of patients, we took advantage of the unique opportunity to study serial changes in tumor acetylation status and gene expression following HDACi administration by performing repeated tumor biopsies at short time intervals, something not possible in patients with systemic or internal tumors. Moreover, this was a group of patients who showed responses to the HDACi therapy.

HDACi are promising new agents for the treatment of hematologic malignancies and possibly solid tumors. To date, results from clinical trials using structurally diverse HDACi, including phenylbutyrate, valproic acid, vorinostat, MS-275, CI-994, PXD-101, AN-9, and MGCD-0103, have been published (13). In general, these agents can be safely administered with class-related toxicities including transient cytopenia, nausea, diarrhea, somnolence, fatigue, and QTc prolongation, which appear to be schedule, route, and dose dependent (13). Romidepsin (17, 31) and vorinostat (19) have shown activity in CTCL; indeed, vorinostat was recently approved by the U.S. Food and Drug Administration for the treatment of cutaneous manifestations in patients with CTCL who have progressive, persistent, or recurrent disease on or following two systemic therapies (32). Panobinostat is a cinnamic hydroxamic acid HDACi that can kill primary chronic myelogenous leukemia, acute myelogenous leukemia, and multiple myeloma cells *in vitro* (14, 33–35). In a phase I study in leukemia and

myeloproliferative disorders, panobinostat administered orally has produced objective responses (36).

Oral panobinostat showed antitumor effects with 6 of 10 patients responding using stringent CTCL-specific response criteria, including 2 patients with disease progression while on panobinostat who attained complete remissions several weeks after discontinuation of therapy. The median time to response was 60 days. The median duration of therapy was 14 weeks, with 1 patient receiving therapy for 29 months. Thus, panobinostat can now be added to the list of HDACi with demonstrable benefit in T-cell lymphomas along with vorinostat (19) and romidepsin (17, 31).

Based on previous studies conducted with HDACi, it has been hypothesized that the primary molecular mechanisms of action by HDACi were to alter the acetylation status of the core histone proteins, thus facilitating chromatin remodeling and its consequent alterations in gene expression (9). The baseline level of acetylation assessed in our patient tumor samples was relatively low. Because of the unique design of this study, whereby we serially sampled tumor specimens following drug dosing, we then assessed tumoral acetylation changes over the first 24 h. Following the administration of panobinostat, we observed rapid acetylation of histone H3, suggesting that early acetylation of histones may be an important mechanism required for the action of panobinostat in patients. The changes paralleled that observed in the peripheral blood mononuclear cells; indeed, in peripheral blood mononuclear cells, hyperacetylation was observed to 72 h, the longest gap between drug dosing. Bearing in mind the small number of patients in the study, there was no observable relationship with peripheral blood mononuclear cell acetylation status and disease response.

Again, the unique design of this study allowed us to gain insight into the alteration in gene expression in tumor cells over time following administration of a HDAC. Early induction of histone acetylation was concomitant with observed alterations in gene expression. Altered gene expression within 4 h of treatment with panobinostat occurred in all patients with <10% of genes altered, which is consistent to that observed in various tumor cell lines (29, 37). Of note, most patients showed a time-dependent decrease in gene expression in the majority of differentially expressed genes, with only patient 104 showing more genes up-regulated in response to panobinostat. Moreover, most of the genes showed peak altered expression at the 4-h time point, indicating that future gene profiling studies using samples from patients treated with panobinostat could be done at the early time point. Due to the relatively low patient numbers, it was not possible to correlate altered expression of a particular gene(s) with patient outcome.

A collective study was also done to investigate genes that move consistently over time in all patients. Our study design allowed a rigorous statistical analysis adjusting for differences between the patients and variations in precision between the RNA samples. A total of 23 genes showed statistical signifi-

cance. From these collected data, 4 genes were further selected for validation by QRT-PCR. Duvic et al. recently showed that treatment of CTCL patients with vorinostat resulted in altered expression of TSP-1, a potent inhibitor of angiogenesis (19). Likewise, CTCL patients receiving panobinostat displayed down-regulation of guanylate cyclase 1A3 (GUCY1A3) that when down-regulated by small interfering RNA results in reduced angiogenic activity (38). The proangiogenic gene *ANGPT1* was another gene consistently down-regulated in response to panobinostat. Down-regulation of *ANGPT1* in response to other small-molecule anticancer agents such as bortezomib has been proposed to play an important anticancer role for this agent in multiple myeloma (39). Finally, the transcription factor COUP-TFII (*NR2F2*), which is an upstream regulator of genes including *ANGPT1*, *hTERT*, and *CCND1* and has been shown to regulate cell cycle progression (40) and angiogenesis (41), was down-regulated in response to panobinostat. Whether the panobinostat-mediated changes in expression of *ANGPT1* and *CCND1* occur as a consequence of altered expression of *NR2F2* remains to be determined. *CCND1* is a gene commonly down-regulated by various HDACi (42), and given the important oncogenic role of cyclin D1 due to its ability to regulate cell cycle progression (43), the significance of down-regulation of *CCND1* for the therapeutic activities of panobinostat should be assessed in more detail.

Panobinostat achieves clinical responses in CTCL at a dose of 20 mg MWF each week, including complete responses and responses that in some patients can be prolonged. The unique design of this study allowed us to monitor tumor gene expression over time. The correlative data suggest that the antiangiogenic, immune modulation, and apoptotic properties of panobinostat shown by distinct changes in gene expression may underpin the observed clinical response in CTCL patients. Although these results offer a possible explanation to the molecular mechanisms underlying patient response to panobinostat, a greater implication could be the possible identification of biomarkers as these genes have shown to respond to panobinostat in all patients, although a larger study for further investigation is still required.

Disclosure of Potential Conflicts of Interest

Acknowledgments

References

1. Willemze R, Jaffe ES, Burg G, et al. WHO-EORTC classification for cutaneous lymphomas. Blood 2005;105: 3768–85.
2. Kashani-Sabet M, McMillan A, Zackheim HS. A modified staging classification for cutaneous T-cell lymphoma. J Am Acad Dermatol 2001;45:700–6.
3. Querfeld C, Rosen ST, Guitart J, Kuzel TM. The spectrum of cutaneous T-cell lymphomas: new insights into biology and therapy. Curr Opin Hematol 2005;12: 273–8.
4. Marks PA, Breslow R. Dimethyl sulfoxide to vorinostat: development of this histone deacetylase inhibitor

as an anticancer drug. Nat Biotechnol 2007;25: 84–90.

5. Duvic M, Hymes K, Heald P, et al. Bexarotene is effective and safe for treatment of refractory advanced-stage cutaneous T-cell lymphoma: multinational phase II-III trial results. J Clin Oncol 2001;19: 2456–71.

6. Olsen E, Duvic M, Frankel A, et al. Pivotal phase III trial of two dose levels of denileukin diftitox for the treatment of cutaneous T-cell lymphoma. J Clin Oncol 2001;19:376–88.

7. Kim EJ, Hess S, Richardson SK, et al. Immunopathogenesis and therapy of cutaneous T cell lymphoma. J Clin Invest 2005;115:798–812.

8. Prince HM, McCormack C, Ryan G, O'Keefe R, Seymour JF, Baker C. Management of the primary cutaneous lymphomas. Australas J Dermatol 2003; 44:227–40; quiz 41–2.

9. Bolden JE, Peart MJ, Johnstone RW. Anticancer activities of histone deacetylase inhibitors. Nat Rev Drug Discov 2006;5:769–84.

10. Baylin SB, Ohm JE. Epigenetic gene silencing in cancer—a mechanism for early oncogenic pathway addiction? Nat Rev Cancer 2006;6:107–16.

11. Lund AH, van Lohuizen M. Epigenetics and cancer. Genes Dev 2004;18:2315–35.

12. Pandolfi PP. Histone deacetylases and transcriptional therapy with their inhibitors. Cancer Chemother Pharmacol 2001;48 Suppl 1:S17–9.

13. Rasheed WK, Johnstone RW, Prince HM. Histone deacetylase inhibitors in cancer therapy. Expert Opin Investig Drugs 2007;16:659–78.

14. George P, Bali P, Annavarapu S, et al. Combination of the histone deacetylase inhibitor LBH589 and the hsp90 inhibitor 17-AAG is highly active against human CML-BC cells and AML cells with activating mutation of FLT-3. Blood 2005;105:1768–76.

15. Kelly WK, O'Connor OA, Krug LM, et al. Phase I study of an oral histone deacetylase inhibitor, suberoylanilide hydroxamic acid, in patients with advanced cancer. J Clin Oncol 2005;23:3923–31.

16. O'Connor OA, Heaney ML, Schwartz L, et al. Clinical experience with intravenous and oral formulations of the novel histone deacetylase inhibitor suberoylanilide hydroxamic acid in patients with advanced hematologic malignancies. J Clin Oncol 2006;2:166–73.

17. Piekarz RL, Robey R, Sandor V, et al. Inhibitor of histone deacetylation, depsipeptide (FR901228), in the treatment of peripheral and cutaneous T-cell lymphoma: a case report. Blood 2001;98:2865–8.

18. Zhang C, Richon V, Ni X, Talpur R, Duvic M. Selective induction of apoptosis by histone deacetylase inhibitor SAHA in cutaneous T-cell lymphoma cells:

relevance to mechanism of therapeutic action. J Invest Dermatol 2005;125:1045–52.

19. Duvic M, Talpur R, Ni X, et al. Phase 2 trial of oral vorinostat (suberoylanilide hydroxamic acid, SAHA) for refractory cutaneous T-cell lymphoma (CTCL). Blood 2007;109:31–9.

20. Prince HM, George DJ, Patnaik A, et al. Phase I study of oral LBH589, a novel deacetylase (DAC) inhibitor in advanced solid tumors and Non-Hodgkin's lymphoma [abstract 3500]. J Clin Oncol 2007;25.

21. Bolstad BM, Collin F, Brettschneider K, et al. Quality assessment of Affymetrix GeneChip data. In: Gentleman R, Carey V, Dudoit S, Irizarry R, Huber W, editors. Bioinformatics and computational biology solutions using R and bioconductor. New York: Springer; 2005. p. 33–47.

22. Wu Z, Irizarry RA, Gentleman R, Martinez-Murillo F, Spencer F. A model-based background adjustment for oligonucleotide expression arrays. J Am Stat Assoc 2004;99:909–17.

23. Smyth GK. Limma: linear models for microarray data. In: Gentleman R, Carey V, Dudoit S, Irizarry R, Huber W, editors. Bioinformatics and computational biology solutions using R and bioconductor. New York: Springer; 2005. p. 397–420.

24. Ritchie ME, Diyagama D, Neilson J, et al. Empirical array quality weights in the analysis of microarray data. BMC Bioinformatics 2006;7:261.

25. Smyth GK. Linear models and empirical Bayes methods for assessing differential expression in microarray experiments. Stat Appl Genet Mol Biol 2004;3:Article 3.

26. Benjamini Y, Hochberg Y. Controlling the false discovery rate: a practical and powerful approach to multiple testing. J R Stat Soc Series B 1995;57:289–300.

27. Gough DJ, Sabapathy K, Ko EY, et al. A novel c-Jun-dependent signal transduction pathway necessary for the transcriptional activation of interferon γ response genes. J Biol Chem 2007;282:938–46.

28. Sandor V, Senderowicz A, Mertins S, et al. P21-dependent g(1)arrest with downregulation of cyclin D1 and upregulation of cyclin E by the histone deacetylase inhibitor FR901228. Br J Cancer 2000;83: 817–25.

29. Mitsiades CS, Mitsiades NS, McMullan CJ, et al. Transcriptional signature of histone deacetylase inhibition in multiple myeloma: biological and clinical implications. Proc Natl Acad Sci U S A 2004;101:540–5.

30. Richon VM, Sandhoff TW, Rifkind RA, Marks PA. Histone deacetylase inhibitor selectively induces p21WAF1 expression and gene-associated histone acetylation. Proc Natl Acad Sci U S A 2000;97: 10014–9.

31. Piekarz R, Frye R, Wright J, et al. Update of the NCI multiinstitutional phase II trial of romidepsin, FK228, for patients with cutaneous or peripheral T-cell lymphoma [abstract 8027]. J Clin Oncol 2007;25.

32. Marks PA. Discovery and development of SAHA as an anticancer agent. Oncogene 2007;26:1351–6.

33. Fiskus W, Pranpat M, Bali P, et al. Combined effects of novel tyrosine kinase inhibitor AMN107 and histone deacetylase inhibitor LBH589 against Bcr-Abl-expressing human leukemia cells. Blood 2006;108: 645–52.

34. Maiso P, Carvajal-Vergara X, Ocio EM, et al. The histone deacetylase inhibitor LBH589 is a potent anti-myeloma agent that overcomes drug resistance. Cancer Res 2006;66:5781–9.

35. Catley L, Weisberg E, Kiziltepe T, et al. Aggresome induction by proteasome inhibitor bortezomib and α-tubulin hyperacetylation by tubulin deacetylase (TDAC) inhibitor LBH589 are synergistic in myeloma cells. Blood 2006;108:3441–9.

36. Kalff A, Shortt J, Farr J, et al. Laboratory tumor lysis syndrome complicating LBH589 therapy in a patient with acute myeloid leukaemia. Haematologica 2008; 93:e16–7.

37. Peart MJ, Smyth GK, van Laar RK, et al. Identification and functional significance of genes regulated by structurally different histone deacetylase inhibitors. Proc Natl Acad Sci U S A 2005;102:3697–702.

38. Saino M, Maruyama T, Sekiya T, Kayama T, Murakami Y. Inhibition of angiogenesis in human glioma cell lines by antisense RNA from the soluble guanylate cyclase genes, GUCY1A3 and GUCY1B3. Oncol Rep 2004;12: 47–52.

39. Roccaro AM, Hideshima T, Raje N, et al. Bortezomib mediates antiangiogenesis in multiple myeloma via direct and indirect effects on endothelial cells. Cancer Res 2006;66:184–91.

40. Nakshatri H, Mendonca MS, Bhat-Nakshatri P, Patel NM, Goulet RJ, Jr., Cornetta K. The orphan receptor COUP-TFII regulates G2/M progression of breast cancer cells by modulating the expression/activity of p21 (WAF1/CIP1), cyclin D1, and cdk2. Biochem Biophys Res Commun 2000;270:1144–53.

41. Pereira FA, Qiu Y, Zhou G, Tsai MJ, Tsai SY. The orphan nuclear receptor COUP-TFII is required for angiogenesis and heart development. Genes Dev 1999;13:1037–49.

42. Johnstone RW. Histone-deacetylase inhibitors: novel drugs for the treatment of cancer. Nat Rev Drug Discov 2002;1:287–99.

43. Tashiro E, Tsuchiya A, Imoto M. Functions of cyclin D1 as an oncogene and regulation of cyclin D1 expression. Cancer Sci 2007;98:629–35.

Clinical Cancer Research

Histone Deacetylase Inhibitor Panobinostat Induces Clinical Responses with Associated Alterations in Gene Expression Profiles in Cutaneous T-Cell Lymphoma

Leigh Ellis, Yan Pan, Gordon K. Smyth, et al.

Updated version	Access the most recent version of this article at: http://clincancerres.aacrjournals.org/content/14/14/4500
Supplementary Material	Access the most recent supplemental material at: http://clincancerres.aacrjournals.org/content/suppl/2008/07/15/14.14.4500.DC1

Cited articles	This article cites 39 articles, 18 of which you can access for free at: http://clincancerres.aacrjournals.org/content/14/14/4500.full#ref-list-1
Citing articles	This article has been cited by 29 HighWire-hosted articles. Access the articles at: http://clincancerres.aacrjournals.org/content/14/14/4500.full#related-urls

E-mail alerts	Sign up to receive free email-alerts related to this article or journal.
Reprints and Subscriptions	To order reprints of this article or to subscribe to the journal, contact the AACR Publications Department at pubs@aacr.org.
Permissions	To request permission to re-use all or part of this article, use this link http://clincancerres.aacrjournals.org/content/14/14/4500. Click on "Request Permissions" which will take you to the Copyright Clearance Center's (CCC) Rightslink site.